INIS-mf--13581

TRAINING IN MANAGEMENT AND ANALYSIS OF SEVERE ACCIDENTS

ORGANISED BY FRANCE

IN THE FRAME OF THE
INTERNATIONAL ATOMIC ENERGY AGENCY
TECHNICAL COOPERATION PROGRAM
(HUN/9/013)

BUDAPEST

13 - 24 JANUARY 1992

3 - LWR SEVERE ACCIDENT ANALYSIS
3.3 INTERNATIONAL RESEARCH PROGRAMS RELATED TO SEVERE ACCIDENTS AND ACCIDENT MANAGEMENT

CORE DEGRADATION AND FISSION PRODUCT RELEASE

R. W. WRIGHT - S. J. L. HAGEN

PRESENTED BY A. MEYER-HEINE

CORE DEGRADATION AND FISSION PRODUCT RELEASE

Robert W. Wright
U.S. Nuclear Regulatory Commission
and
Siegfried J.L. Hagen
Kernforschungszentrum Karlsruhe

SUMMARY

Experiments on core degradation and melt progression in severe LWR accidents have provided reasonable understanding of the principal processes involved in the early phase of melt progression that extends through core degradation and metallic material melting and relocation. A general but not a quantitative understanding of late phase melt progression that involves ceramic material melting and relocation has also been obtained, primarily from the TMI-2 core examination. A summary is given of the current state of knowledge on core degradation and melt progression obtained from these integral experiments and of the principal remaining significant uncertainties. A summary is also given of the principal results on in-vessel fission product release obtained from these experiments.

1. OVERVIEW

This paper describes the current state of knowledge on core degradation and in-vessel core-melt progression in LWR core uncovery accidents and gives a summary of the results on in-vessel fission product release from integral in-reactor tests. Melt progression describes the state of an LWR reactor core from core uncovery up to reactor vessel meltthrough in unrecovered accidents, or through temperature stabilization in accidents recovered by core reflooding. Melt progression provides the initial conditions for assessing the core-melt threat to containment integrity, in particular the threat of early containment failure, which, along with the containment bypass sequences, provides the principal contribution to severe accident risk(1). Significant parameters involved here are the melt mass, composition, temperature (superheat), and rate of release from the vessel. Melt progression provides the in-vessel hydrogen generation and the conditions that govern the in-vessel release of fission products and aerosols and their transport and retention in the primary system. Melt progression also provides the core conditions for assessing accident management strategies. Sensitivity studies have shown that uncertainties regarding melt progression provide major uncertainties in assessing severe accident consequences and risk.

Much has been learned about the processes involved in core degradation, in the early phase of melt progression that extends through metallic (but not ceramic) material melting and relocation, and in in-vessel fission product and aerosol release. This information has come from many integral tests in the PBF, ACRR, NRU, NSRR, and TREAT test reactors, from the LOFT FP-2 test, from the Phebus CSD tests, from tests in the CORA ex-reactor fuel damage test facility, and from separate-effects experiments on significant phenomena. Most of the available information on the late

phase of core-melt progression that involves ceramic material melting and relocation has come from the post-accident examination of the TMI-2 core. Despite the core reflooding that successfully terminated the TMI-2 accident, the general late-phase melt progression phenomenology of that accident appears to be applicable to unrecovered as well as to recovered PWR accidents. If there are any BWR accidents which involve metallic core blockage like that at TMI-2, then this general phenomenology should also be applicable to such accidents. The sources of the current information base on melt progression from integral experiments and an outline of the information obtained from these experiments is given in Table 1.

The results of these integral tests and the TMI-2 core examination have provided a very consistent picture of melt progression(2,3). This picture involves the development of a debris-supporting metallic blockage across the lower core and above the water level during coolant boildown, and is called the blocked-core accident pathway. The TMI-2 core examination has shown that a pool of mostly ceramic melt grows from decay heat in the particulate, mostly ceramic debris bed that is supported by the metallic core blockage. The growing pool melts through the supporting metallic blockage and secondary ceramic crusts that surround the ceramic melt pool, or out the side of the core as happened at TMI-2 with a reflooded core, and the melt then drains into the vessel lower plenum.

The end-state configuration of the TMI-2 core, shown in Figure 1, illustrates the blocked core accident pathway(3). The central region of the core contains refrozen ceramic melt from the undrained portion of the ceramic melt pool. Below this pool is a metallic crust that had previously blocked the core, and above the pool is a mostly ceramic crust. Below the metallic crust are undamaged sections of fuel assemblies that were cooled throughout the accident by water in the bottom of the core. At the side of the core is the drainage pathway through which 20% of the core mass drained into the lower plenum water upon pool meltthrough out the side of the core. Refrozen ceramic melt and solid debris are in the vessel lower head. There was no meltthrough at the metallic downward protuberance near the core axis. Above the pool and upper crust are a mostly ceramic particulate debris bed and a large void produced by subsidence of the bed from debris densification in melting and from drainage of the melt pool. The TMI-2 configuration illustrates essentially all of the detailed melt progression phenomenology thought to apply to blocked core accident sequences in PWRs and also to any BWR accidents that follow blocked core sequences. According to current knowledge, however, it is possible that meltthrough in unrecovered accidents would occur near the core axis causing full drainage of the ceramic melt pool.

A major finding from all the integral tests and also from the TMI-2 core examination is that the unoxidized zircaloy and the control rod materials and their eutectics melt before or during the rapid temperature transient from steam oxidation of the core zircaloy and at temperatures ranging from as low as 1200K for the eutectics up to 2250K for zircaloy(4). A diagram of the threshold temperatures for liquid phase formation for the relevant materials in LWR accidents, both from melting and from eutectic materials interaction, is given in Figure 2(5).

Videotapes of the CORA experiments have shown that metallic melt relocation is essentially a noncoherent, noncoplanar rivulet flow process that is quite different from the coplanar modeling of film flow along the rods that is used in current codes(6). This explains why the developing partial blockages in the PBF and other integral multi-rod tests did not cut off the steam flow and hydrogen generation.

Metallic melt relocation leaves behind free-standing UO_2 fuel pellets and ZrO_2 oxidized cladding shards that have melting points (including eutectics) in the range for 2800K to 3100K. During late-phase melt progression in unrecovered accidents and in very severe recovered accidents such as TMI-2, a ceramic melt pool forms in the mostly ceramic debris bed with further core heatup. Thus the metallic and the ceramic debris with melting points that differ by 600K or more become separated in space, and, as the TMI-2 core examination show, they behave quite differently in continued melt progression. Older simplified codes treat the core melt as a single fictitious "corium" fluid with a unique (high metallic) composition, a relatively low melting point (usually 2550K),and with an assumed fraction of the core mass released as "corium" melt upon an assumed nonmechanistic core "slumping."

BWR core geometry tests in ACRR (DF-4) and CORA have shown that eutectic interactions of the control-blade B_4C powder and their stainless steel sheaths at about 1500 K liquify the blade materials(4). This melt undergoes further eutectic interactions with the zircaloy channel box walls that fail the walls and open up the compartmentalized BWR core geometry. The control-blade materials relocates downward and possibly even out of the core in a BWR accident with potential recriticality problems for core reflooding. In these tests, however, which were all performed for BWR wet core conditions (that is with relatively high steaming rates and relatively cold temperatures in the lower sections of the test bundle), a metallic partial blockage formed at the bottom of the test bundles as in PWR core geometry tests.

This question of metallic melt drainage or core blockage, particularly for BWRs, is a major branch point for in-vessel core melt progression, and it has a large effect upon the characteristics of the melt released from the core into the lower plenum. In the core blockage case, a large mass of mostly ceramic melt at about 3000K drains rapidly into the water filled lower plenum, as happened at TMI-2. In the drainage case, layers of quenched melt are formed under the lower plenum water in the order of their time of melting and drainage from the core, with the low-melting metals at the bottom and the ceramics at the top. These differences also have a major effect on the vessel failure process and on the characteristics of the melt released into the containment upon vessel failure.

2. EXPERIMENTS AND INTERPRETATION ON CORE DEGRADATION AND MELT PROGRESSION

A summary of the conditions for the integral tests that have been performed on core degradation and melt progression (including the TMI-2 accident), mostly taken from Hobbins, et. al., is given in Table 2(4). These tests have covered a wide range of conditions. They involve both open PWR core geometries and the compartmentalized BWR geometries that

have zircaloy channel boxes and B_4C control blades. They range in scale from 8 rods to 100 rods in the test fuel bundles and up to the 36,816 rod TMI-2 core, and from 0.5 meter length to full 4.0 meter core length. The fuel irradiation range includes fresh fuel, trace irradiated fuel, low burnup fuel, and high burnup (30 Gwd/tU) fuel. Fission heating, decay heating, and electrical heating of the test fuel rods have been used. Most of the tests have had boil off steam flow rates, with some tests at higher or lower flow. Both inconel and zircaloy grid spacers have been used. This table does not include the NSRR power excursion tests or the ACRR late-phase melt progression experiments that start from the late-phase debris bed geometry rather than from the initial intact fuel rod geometry. Also not included in the table are small in-reactor separate-effects tests on fission product and aerosol release, four STEP tests in TREAT and two somewhat similar ST tests in ACRR that had a reducing hydrogen environment. These tests all used 4-rod bundles of high burnup BR-3 fuel. The PBF SFD 1-3 and 1-4 tests also used high burnup BR-3 fuel. The NRU FLHT-4 and -5 tests included a single high burnup rod of commercial PWR fuel.

In all of the tests for prototypic coolant boildown conditions, steam oxidation of the uncovered cladding with attendant hydrogen generation became significant at about 1500K and increased the heating rate above the initial 0.5 K/sec prototypic of decay heat. Initially the local oxidation is rate limited by oxygen diffusion through the growing ZrO_2 sheath which gives parabolic kinetics. This process is strongly temperature dependent. At about 1700K the rate of local oxidation heating increases rapidly to tens of K/sec, limited only by conversion of the entire steam flow into hydrogen (steam starvation) and by relocation of unoxidized molten zircaloy downward to cooler regions where it freezes and forms a partial metallic blockage. A burn front moves down the bundle during this process and leaves the hot upper part of the bundle in a reducing hydrogen environment. This has significance for fission-product release and transport and for core reflooding. This reducing environment in the upper part of the core is a transient effect that does not persist except for the general hydrogen build up in the primary system.

In tests that have either stainless-steel clad-Ag-In-Cd PWR control rods in zircaloy guide tubes, stainless-steel clad BWR B_4C control blade in the gaps between zircaloy BWR channel boxes, or inconel grid spacers, the control materials start to liquify and to attack and liquify adjacent zircaloy well below the melting points of the individual materials and well before the start of the rapid oxidation temperature transient. Intact core geometry in reactor accidents is lost from these eutectic interactions at temperatures well below the melting points of the individual materials. Figure 2 shows a chart of the threshold temperatures for liquid phase formation for the relevant materials in LWR accidents, both from melting and from materials interaction eutectics(5). For PWRs, Fe-Zr and Ni-Zr eutectics occur at about 1200K, but in integral core-geometry tests the first eutectic melts (and loss of core geometry) occur at about 1520K. For BWRs, B_4C-Fe eutectics occur at about 1420K, and rapid liquifaction in integral tests occurs at about 1520K. In contrast, the melting point of as-received zircaloy 4 is 2030K and that of oxygen-stabilized alpha zirconium is 2250K. It has also been found in these integral tests that the molten metallic zircaloy dissolves a

significant fraction of the solid UO_2 fuel. This has potential significance for fission product release.

Core degradation experiments in the CORA ex-reactor fuel-damage test facility, the videotapes of the processes involved, and the post test sectioning and examination of the test and bundles have provided the most detailed observations available on core degradation processes(6). Corollary work at KfK has also provided/basic information on the fundamental materials interactions involved in the core-degradation process and on their rate limitations(5).

In the CORA experiments, electrically heated UO_2/Zry-4 fuel rod simulators with absorber rods and spacers are subjected to temperatures up to 2700K in a steam environment. Most of the PWR tests have stainless-steel-clad Ag-In-Cd absorber rods within zircaloy guide tubes, and the BWR tests have B_4C absorber rods in stainless-steel-clad blades in the gap between Zry channel box walls. A schematic drawing of the CORA experimental configuration is shown in Figure 3. The CORA tests are terminated by power reduction with continuing gas flow (slow cooldown) or by flooding with water (fast cooldown).

Most of the information from the CORA tests is obtained by post-test sectioning and metallurgical examination of the test fuel bundles. Shown in Figure 4 are post-test horizontal and axial sections and a bundle photograph for the CORA-5 PWR test which included a PWR stainless-steel-clad Ag-In-Cd control rod inside a zircaloy guide tube. CORA-5 reached a maximum temperature of about 2300K and had a slow cooldown. The cross sections show the tungsten heater rods in the simulated fuel rods (a third of fuel rods do not contain heater rods but are radiation-heated by the adjacent rods), the control rod, the gray relocated metallic melt, and the blacker epoxy filler for sectioning. The general state of the damage, the missing control rod from the central and upper bundle, and the massive partial blockage from the relocated metallic melt are to be noted.

At the end of 1990, two tests with alumina pellets and ten tests with UO_2 had been performed, 7 with PWR and 3 with BWR fuel bundles. Two of the PWR tests and one BWR test were terminated by water flooding. In general, all the tests have demonstrated the competitive processes of cladding oxidation and low temperature melt formation caused by the interactions of zircaloy with the structural materials. After failure of the cladding in PWR bundles, the Ag-In-Cd and the inconel of the grid spacers liquefy cladding zircaloy at far below its melting temperature. The interaction between boron carbide and stainless steel causes liquefaction of the absorber blade in BWR bundles. The resulting melt penetrates the guide tube (PWR) or the zircaloy channel box wall (BWR) and initiates the liquefaction of the zircaloy cladding of the fuel rods. The liquid metallic zircaloy dissolves some of the UO_2 even though it is only a constituent of the melt which is below the normal melting temperature of zircaloy. The major fraction of the metallic melt in the CORA tests relocated downward inside the bundle and froze at locations where the bundle temperature was below the melt freezing temperature to form a large partial blockage. The presence of a spacer grid favors blockage formation, but is not a necessary condition for blockage. In

the water flooding tests, a large increase in the hydrogen generation occurred along with a large local transient temperature increase in the upper part of the bundle. This shows the influence of the strong zircaloy oxidation reaction from the reflood steam.

A major branch point in the melt progression sequence,particularly for BWRs, involves whether a metallic core blockage develops, as occurred at TMI-2, or whether the metallic melt and later the ceramic melt drain from the core (and BWR core plate) when formed. The mechanism of vessel failure and the characteristics of the melt released into the containment upon vessel failure are strongly dependent upon which of these paths is followed. Accordingly, determination of the accident conditions, if any, for which core blockage does not occur is important. In U.S. BWR accidents in which automatic depressurization is actuated, blowdown lowers the water level below the core and core plate so that core heatup occurs in a dry core at a very low steam flow rate. It has been hypothesized that in this case the metallic and later the ceramic melt drain from the core as formed onto the core plate and later into the lower plenum.

Other early (metallic-melt) phase phenomena with potentially significant uncertainties are: the effects of the eutectic interactions of control-rod materials with zircaloy, particularly for BWRs, and of inconel grid spaces with zircaloy; the threshold mechanism (not just the melting point) for zircaloy melt relocation in fuel-rod geometry; oxidation and hydrogen generation from relocating and relocated metallic melts; and the effects of high burnup fuel. Research is currently underway in these areas.

A most important current uncertainty regarding in-vessel melt progression is the failure threshold and the failure location of the debris-supporting metallic crust (and also the secondary ceramic crust) under attack by the growing molten ceramic pool in blocked core accident sequences. These determine the mass of ceramic melt released from the core into the vessel lower plenum and also the composition and the temperature (superheat) of the melt. Resolution of this uncertainty involves experiments and analytical modeling of the dynamics of debris bed melting and of crust relocation and failure.

There are other late (ceramic-melt) phase phenomena that have potentially significant uncertainties. There is a question of whether the blocked core scenario may develop from the growth of the ceramic crust that surrounds the growing melt pool in the particulate mostly ceramic debris-bed in the core region regardless of whether a metallic blockage has previously formed. There are uncertainties regarding the natural circulation thermal hydraulics in the growing ceramic melt pool at prototypic Rayleigh numbers and with turbulent flow, and also uncertainties regarding the time constant for flow start up. There is uncertainty as to whether or not declad high burnup fuel naturally fragments into debris-bed geometry, whether the transition occurs by gravity collapse of an unstable array of free-standing declad fuel rods, or whether core reflooding as occurred at TMI-2 is necessary to produce true debris-bed geometry. There is also uncertainty regarding the rate of oxidation of the remaining metal in the debris bed and its supporting metallic crust (but not in the melt pool itself), although this rate

cannot be large.

A summary of the current state of phenomenological understanding of melt progression is given in Table 3. The table summarizes those phenomena that are reasonably well understood as well as those for which we have a more general understanding.

3. SUMMARY OF FISSION PRODUCT RELEASE IN INTEGRAL TESTS

Information on in-vessel fission product release and aerosol generation has been obtained from the integral tests in PBF with both high-burnup fuel and with trace-irradiated fuel, from the full length FLHT-4 and 5 tests in NRU that included a high burnup commercial PWR fuel rod, from the LOFT FP-2 integral test with low-burnup fuel, from post-accident examination of the TMI-2 core which had low-burnup fuel, from in-reactor fission product and aerosol release experiments with high-burnup fuel in TREAT (the STEP tests) and ACRR (the ST tests), from ex-reactor single-rod integral experiments at Oak Ridge and at Grenoble, and from laboratory separate effects experiments at Whiteshell, Battelle, and other laboratories. This discussion will be limited to a summary of the principal results from the integral in-reactor tests that have been presented previously, primarily as given by Hobbins et. al.(4). A summary of the conditions for these integral tests, including the fuel burnup, is given in Table 2. High-burnup fuel from the BR-3 reactor that will be used in the Phebus FP tests has also been used in the PBF-SFD 1-3 and 1-4 tests, the four TREAT STEP tests, and the two ACRR ST tests in a reducing hydrogen environment. For these tests, the nominal burnup of the BR-3 fuel was 30 Gwd/tU. The fuel at TMI-2 had a burnup of 3 Gwd/tU and that in the LOFT FP-2 test had 0.45 Gwd/tU.

A principal result of the PBF high-burnup fuel tests was that the release rates of the noble and volatile fission products was highly dependent on the changing fuel morphology during core degradation and melt progression, and that these rates were not a unique function of fuel temperature, as sometimes represented(4). This result is illustrated in Figure 5 which shows the fractional release rate of the noble gases and the calculated cladding temperature near the core center as a function of time for the PBF 1-4 test. The fractional release rate of the volatiles was nearly constant at about.0 1 %/sec for a period of about 30 minutes, although the mid-core temperature varied from 2200K to 3000K and back to 2200K during this period, and the rate then fell slowly as the fuel cooled further. This test had four PWR stainless-clad Ag-In-Cd control rods in zircaloy guide tubes in the 32 rod (total) test fuel bundle. The PBF results show that accurate prediction of the fission product release rate depends on knowledge of the state of degradation of the core and of the fuel itself. Potentially significant effects here include fuel cracking, fuel dissolution in molten zircaloy, and whether the environment is oxidizing or reducing.

In the PBF tests and in the TMI-2 core examination, tellurium was found to be retained preferentially in the unoxidized zircaloy, and not released into the gas stream. This retained tellurium is then a

potential source for later ex-vessel release by zirconium oxidation in melt-concrete and melt-coolant interactions.

The TMI-2 core examination showed that from 3% to 10% of the cesium and iodine were retained in the molten ceramic melt in the core and the vessel lower head. Large fractions of the medium and low volatility fission products were also retained in the ceramic melt and in metallic inclusions in the melt. The cerium and strontium were retained in the ceramic melt as oxides, and a large fraction of the antimony, ruthenium, and tellurium were retained in nickel-based metallic inclusions in the ceramic melt. In the upper particulate mostly ceramic debris bed in TMI-2 that had not melted, the retention was about 20% for the volatile cesium and iodine, about 50% for the less volatile metals antimony and ruthenium, and nearly 100% for the low volatility oxides of strontium and cerium.

The LOFT FP-2 test was performed with a large 100-rod test fuel bundle which was irradiated in the reactor to 0.45 Gwd/tU burnup. The bundle also had PWR Ag-In-Cd control rods(7). The test was unique (except for TMI-2) in that the test fuel bundle was heated by fission-product decay. The test was terminated by reflooding with borated water. The principal addition to the PBF fission-product results from the LOFT FP-2 test was that while 3% of the volatile fission product inventory was released during the rapid oxidation transient to about 2200K when reflood was initiated, about 12% of the inventory was released during and after reflood. The reflood steam produced rapid local oxidation of unoxidized zircaloy in the upper part of the core. During the reflood transient, local regions reached UO_2 melting (3100K), and this local heating during reflooding produced most of the hydrogen generation and most of the fission product release in the test.

Two ST separate-effects experiments were performed in ACRR on fission product release from high burnup fuel in the local reducing hydrogen environment that results from steam starvation during the rapid oxidation transient(8). In these tests, large solid-state swelling of the fuel occurred that closed the cooling channels between the rods. These tests used a 4-rod fuel bundle that contained 15 cm sections of fresh fuel as a nuclear preheater followed by 15 cm sections of 30,000 MWd/tU BR-3 test fuel. The high-burnup sections were maintained for 20 minutes at about 2500K, which is well below the melting point of UO_2 but above that of zircaloy. Similar large swelling of high burnup fuel without melting has been observed in the PIE of the steam-starved section of the NRU FLHT-2 test. This phenomena is qualitatively understood in terms of reduction of the UO_2 to metallic uranium at the grain boundaries, liquefaction and fluidization of the UO_2 grains, and fission gas pressurization to produce the fuel swelling. The range of this effect in accident parameter space and its significance for fission product release and melt progression itself are not currently understood. No strong effects of the reducing hydrogen environment upon the fission-product release rates were observed. In the ACRR DF experiments, a dense tin aerosol was observed when the zircaloy cladding melted.

4. ACKNOWLEDGEMENTS

The authors are indebted to Drs. Richard R. Hobbins and David A. Petti for discussions and for information in the paper on the results on in-vessel fission product release in integral in-reactor tests that we gratefully acknowledge.

REFERENCES

1. NUREG-1150, "Severe Accident Risks: An assessment for Five U. S. Nuclear Power Plants," (December, 1990).

2. J. M. Broughton, P. Kuan, D. A. Petti, and E. L. Tolman, "A Scenario of the Three Mile Island Unit 2 Accident," Nucl. Tech. 87, p. 34 (August 1989).

3. R. W. Wright, "Melt Progression Modeling Implications of the TMI-2 Accident," Proc. ICHMT Int. Seminar on 'Fission Product Transport Processes in Reactor Accidents,' Dubrovnik, Yugoslavia (May 22-28, 1989).

4. R. R. Hobbins, D. A. Petti, D. J. Osetek, and D. L. Hagrman, "Review of Experimental Results on LWR Core Melt Progression," Nucl. Tech. (to be published 1991).

5. P. Hofmann, S. Hagen, G. Schanz, and A. Skokan, "Reactor Core Materials Interactions at Very High Temperatures," Nucl. Tech., 87, p. 146 (August, 1989).

6. S. Hagen, P. Hofmann, G. Schanz, and L. Sepold, "Results of the CORA Experiments on Severe Fuel Damage With and Without Absorber Material," Proc. 26th National Heat Transfer Conf., Philadelphia, August 6-9, 1989, AICHE Symposium Series 269, Vol. 85 (1989).

7. M. L. Carboneau, V. T. Berta, and M. S. Modro, "Experiment Analysis and Summary Report for the OECD LOFT Project Fission Product Experiment LP-FP-2," OECD LOFT-T-3806, OECD (June, 1989).

8. M. D. Allen, H. W. Stockman, K. O. Reil, J. W. Fisk, "Fission Product Release and Fuel Behavior of Irradiated Light Water Reactor Fuel Under Severe Accident Conditions: The ST-1 Experiment, NUREG/CR-5345, SAND 89-0308, (to be published 1991).

TABLE 1
Sources of Current Integral Experimental Information

DATA SOURCE	KEY INFORMATION
PBF Severe Fuel Damage Tests: SFD-ST, 1-1, 1-3, 1-4	Integral information base on core degradation and melt progression
ACRR Damaged Fuel Tests: DF-1, -2, -3, -4	Phenomenological information on core degradation and melt progression
NRU Full-length Tests: FLHT 1, 2, 4, 5	Data on length effects, lack of cut off to hydrogen generation, and high burn-up fuel swelling
CORA Ex-reactor Tests: 9 PWR Tests 3 BWR Tests Related Experiments	Basic information base on material-interaction effects and metallic melt relocation Information for BWR & PWR geometries, including reflood effects, using electrically-heated, simulated fuel-rod bundles up to 59 rods
Phebus SFD Tests	Phenomenological information on core degradation processes
LOFT FP-2 Large-Bundle (101-rod) Test	Unique data on metallic melt relocation and lack of hydrogen cutoff with a large flow-bypass area Significant results on reflood effects on melt progression Unique results with fission-product decay heating
ACRR Late Phase (Ceramic Melt) Tests	Dry UO_2 debris-bed melting characteristics Dynamics of pool growth in ceramic debris beds
TMI-2 Core Examination	Major source of significant information on late-phase melt progression Results applicable to basic phenomenology for both recovered & unrecovered accidents

TABLE 2. SUMMARY OF CONDITIONS FOR INTEGRAL TESTS AND THE TMI-2 ACCIDENT

Test/ (Accident)	Fuel Rods	Length (m)	Irradiation (Gwd/tU)	Control Matls.	Heating	System Pres. (MPa
PBF						
SFD-ST	32	0.9	Trace	None	Fission	6.9
SFD 1-1	32	0.9	Trace	None	Fission	6.8
SFD 1-3	28	1.0	36	None	Fission	6.8/4.7
SFD 1-4	28	1.0	36	Ag-In-Cd	Fission	6.95
ACRR						
DF-1	9	0.5	Trace	None	Fission	0.28
DF-2	9	0.5	Trace	None	Fission	1.72
DF-3	8	0.5	Trace	Ag-In-Cd	Fission	0.62
DF-4	14	0.5	Trace	B_4C	Fission	0.69
PHEBUS SFD						0.5,3.5
B9	21	0.8	Trace	None	Fission	
B9R	21	0.8	Trace	None	Fission	
C3	21	0.8	Trace	None	Fission	
AIC	21	0.8	Trace	None	Fission	
CORA						
9 PWR Tests	24, 52	1.0	None	Ag-In-Cd	Electric	0.2,1.0
3 BWR Tests	18, 48	1.0	None	B_4C	Electric	0.2
NRU						
FLHT-1	12	4.0	Trace	None	Fission	1.38
FLHT-2	12	4.0	Trace	None	Fission	1.38
FLHT-4	11	4.0	1-30, 10-Trace	None	Fission	1.38
FLHT-5	11	4.0	1-30, 10-Trace	None	Fission	1.38
LOFT FP-2	100	1.7	0.45	Ag-In-Cd +H_3BO_3	Decay	1.1
TMI-2	36,816	4.0	3	Ag-In-Cd +H_3BO_3	Decay	5-15

Table 3 Core Degradation and Melt Progression:
Status of Current Understanding

Reasonably Well Understood Phenomena in Early (Metallic Melt) Phase

- Clad ballooning
- Intact-core-geometry oxidation heating and hydrogen generation
- UO_2 liquefaction (dissolution) by molten Zircaloy
- Eutectic material interactions and rates among UO_2, ZRO_2, Zry, and control materials and their oxides
- Opening up of the compartmentalized BWR core early in a BWR accident by the eutectic interaction of control-blade material with Zry channel box walls
- Molten Zry relocation is a noncoherent, noncoplanar, rivulent-flow process that does not block steam flow and hydrogen generation. It is not a film flow process

General Understanding of Late (Ceramic Melt) Phase

- Based primarily on TMI-2 core examination
- Results also generally applicable to PWR unrecovered accidents
- Ceramic melt pool growth and meltthrough from block core
- Limited melt mass released from core

Hydrogen Generation and Strong Heating of Uncovered Core from Zircaloy Oxidation by Reflood Steam (LOFT FP-2 and CORA)

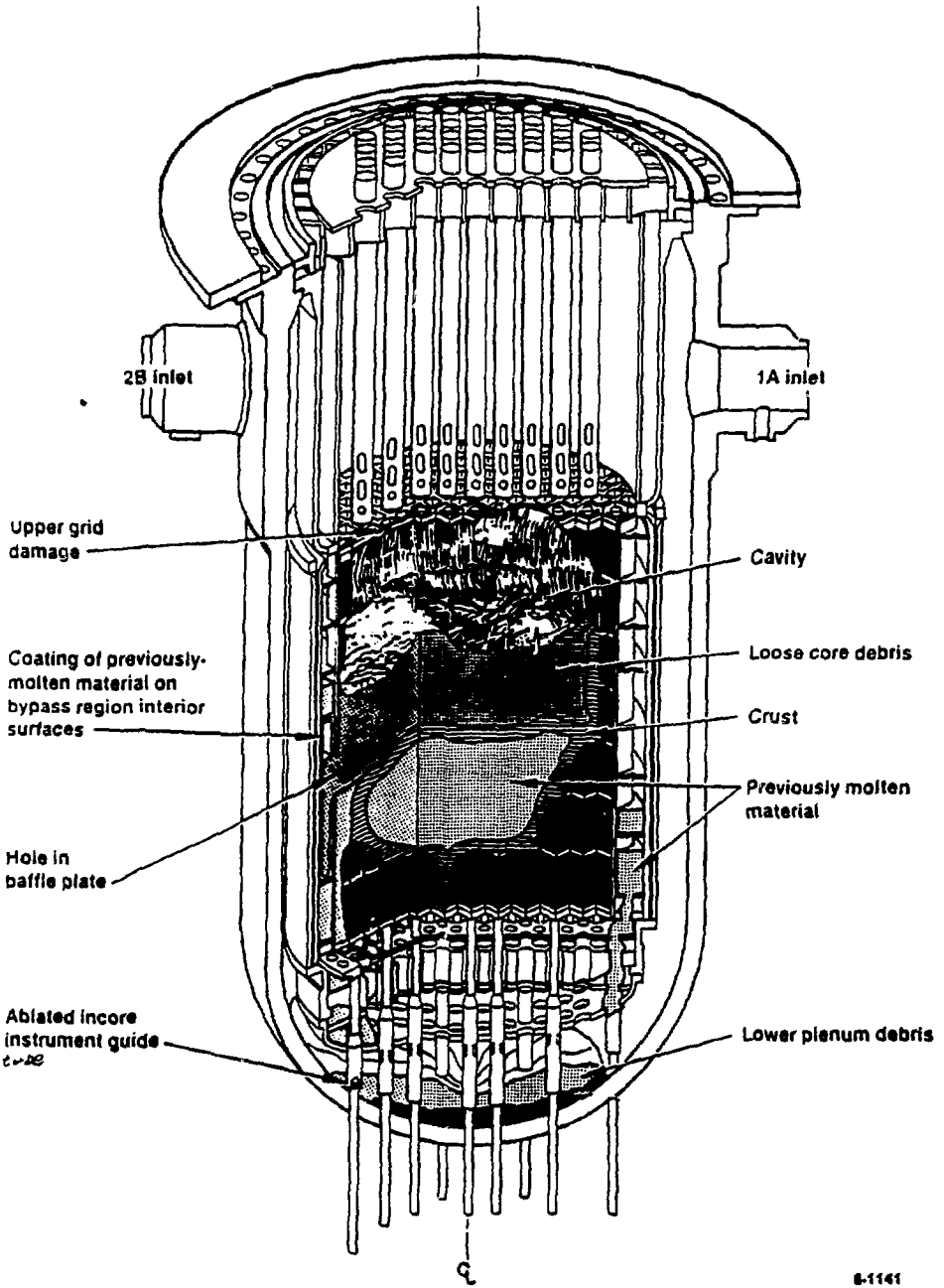

Fig. '. TMI-2 Core End State Configuration

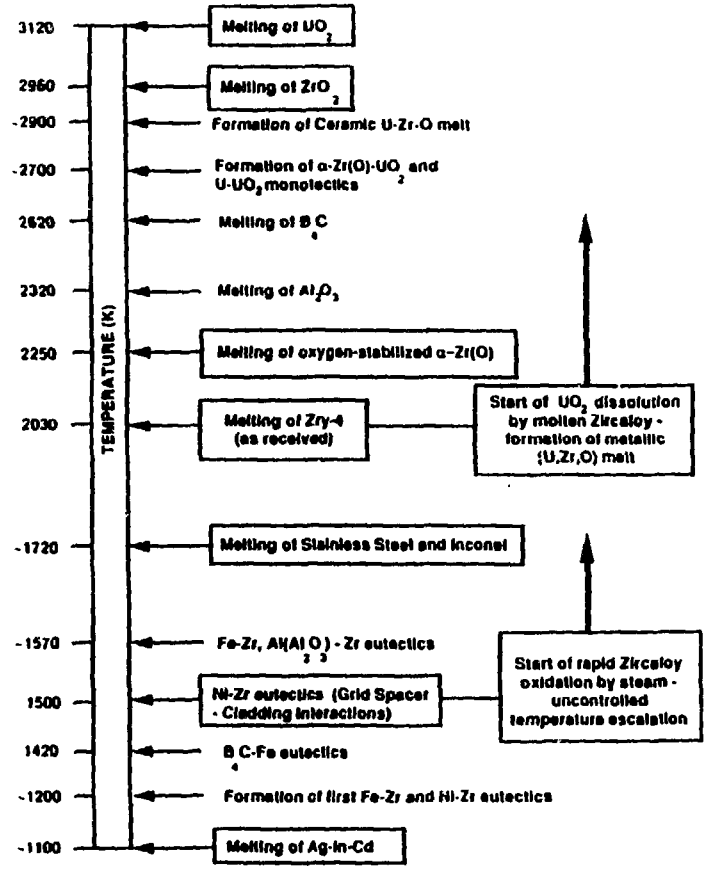

Fig. 2. LWR Severe Accident Relevant Liquid Phase Formation Temperatures

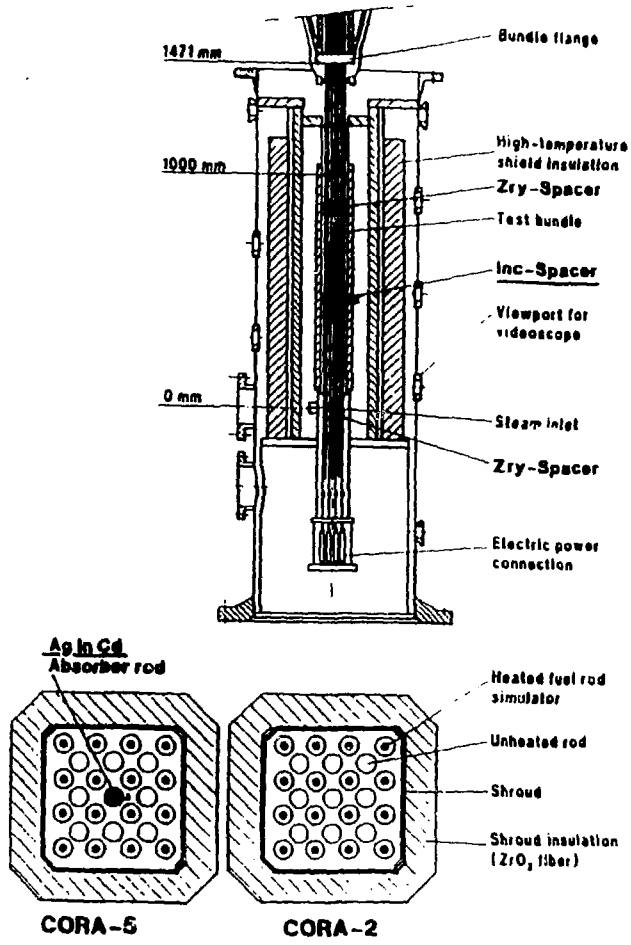

Fig. 3. CORA Experiment Configuration (PWR)

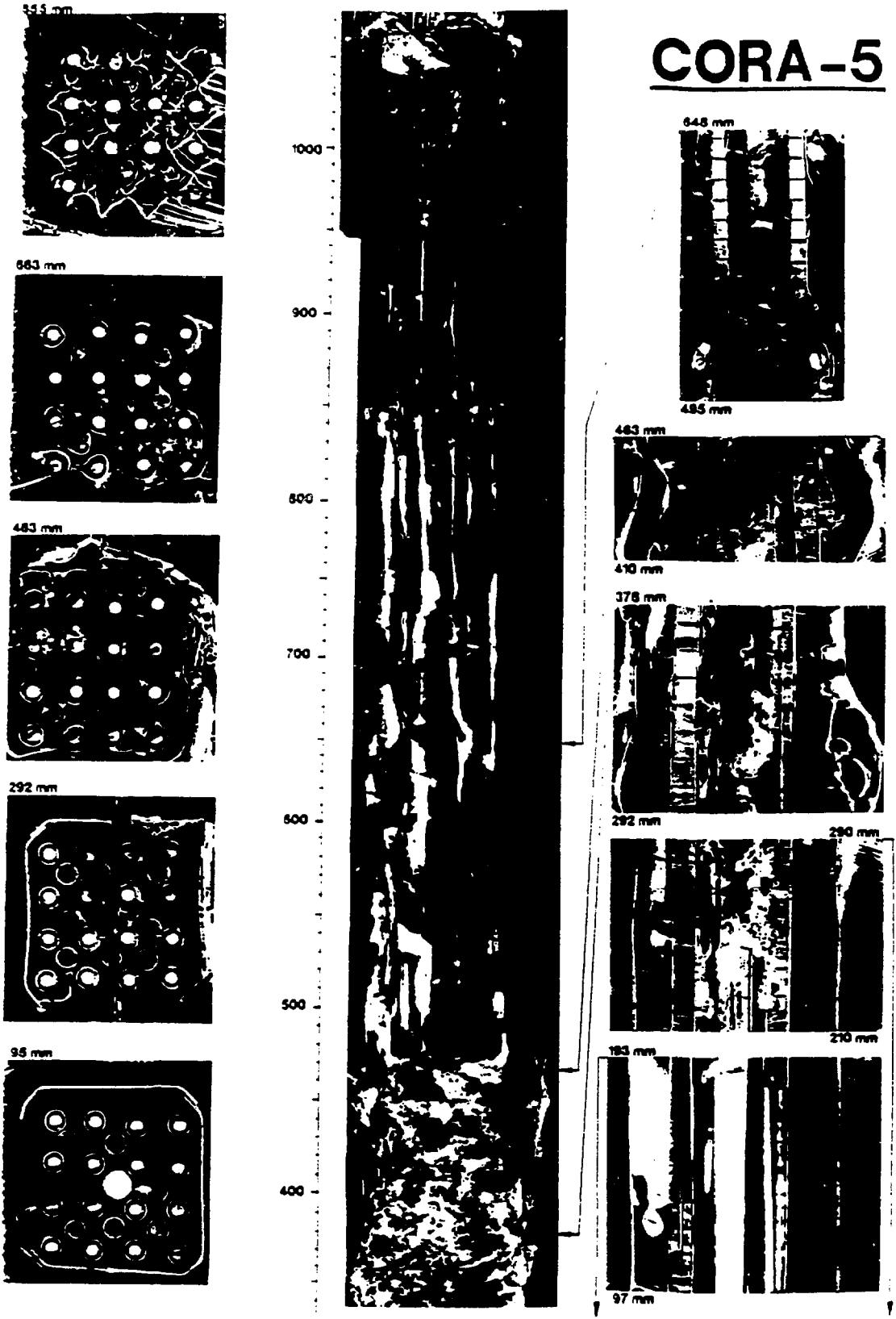

Fig. 4. Horizontal and Vertical Sections of the CORA 5 (PWR) Test Bundle

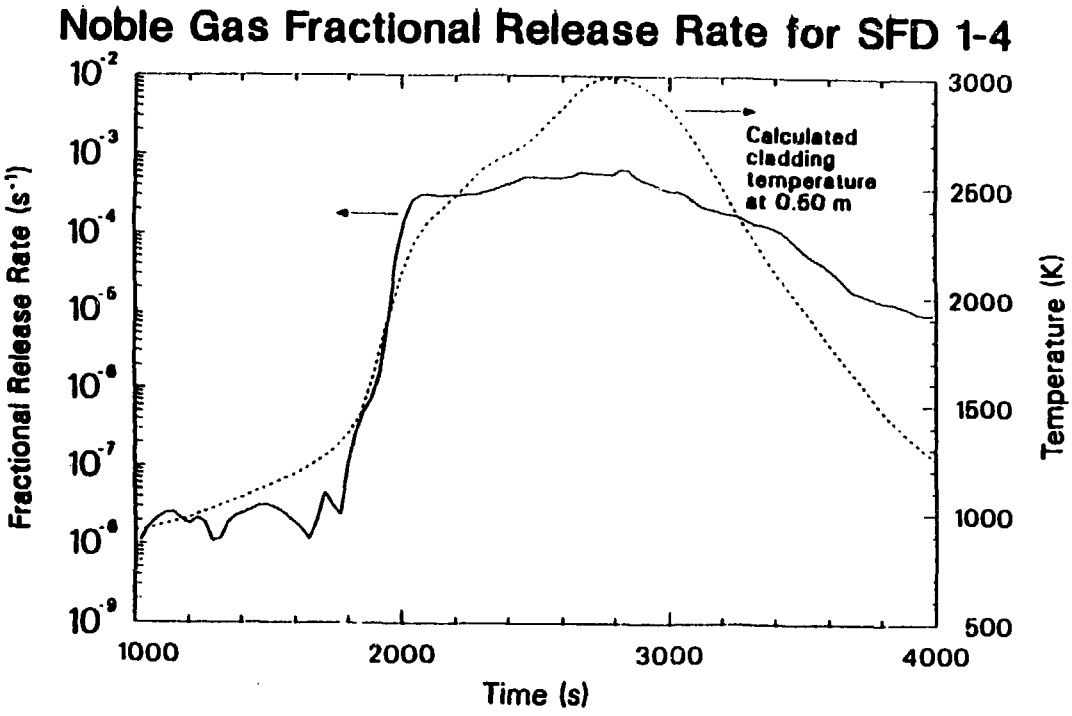

Fig. 5. PBF SFD1-4 Noble Gas Fractional Release Pate and Clad Temperature